# Theoretical Analysis of the Unimolecular Gas-Phase Decompositions of the Propane Molecular Ion

**David J. McAdoo,*,† Santiago Olivella,*,‡,§,⊥ and Albert Solé‡**

*Marine Biomedical Institute, University of Texas Medical Branch, Galveston, Texas 77555-1069, Departaments de Química Orgànica i Química Física, Universitat de Barcelona, Martí i Franquès 1, 08028 Barcelona, Catalunya, Spain, and the Departament de Química Orgànica Biològica, CSIC, Jordi Girona 18, 08034-Barcelona, Catalunya, Spain*

*Received: July 2, 1998; In Final Form: October 27, 1998*

Although the propane ion has been a long-standing model for RRKM/QET calculations, the validity of the transition states utilized in such calculations was unclear. To remedy this, we use potential energy barriers and harmonic vibrational frequencies calculated at the ab initio QCISD(T)/6-311+G(2d,2p) and UMP2/6-31G(d) levels of theory, respectively, as parameters to compute rate constants versus internal energy curves for the losses of the H atom, $CH_3^{\bullet}$, and $CH_4$ from the propane ion by a RRKM procedure. The results agree reasonably with experimental ones. The ab initio calculations confirm that H atom loss occurs from the middle carbon of the propane ion to form the *sec*-propyl cation. The rate constant of H atom loss increases slowly with increasing internal energy, which is surprising for a simple bond cleavage. This is shown to be due to the changes in vibrational frequencies between the propane ion and the transition state being small for this reaction. Methane elimination occurs in a stepwise fashion through a methyl radical−ethyl ion complex. Low frequencies arising from CC bond elongation in the rate determining step for this reaction give a faster rise in rate constant with increasing internal energy for this reaction than for H atom loss, despite the former reaction being an elimination. A number of frequencies are very low in the transition state for $CH_3^{\bullet}$ loss, taken to be a loosely bound methyl radical−ethyl ion complex. This gives a very rapid rise in the rate constant of this simple CC bond cleavage with increasing internal energy. Losses of single atoms by simple cleavages are predicted to be slower than most types of competing reactions due to changes in vibrational frequencies between the reactant and transition states being relatively small.

## Introduction

The propane ion ($C_3H_8^{+\bullet}$) has been a favorite model for developing theoretical descriptions of the unimolecular decompositions of ions in the gas phase since Rosenstock and co-workers[1] used it to introduce the quasi-equilibrium theory (QET), an approach that became highly successful in describing the dissociations of ions in the gas phase. A number of subsequent studies[2−4] utilized ionized propane as a model for testing and/or developing the QET, but each invoked arbitrary assumptions regarding the reactant and transition state vibrational frequencies.

In 1960, Kropf and co-workers[2] used the QET to "reasonably" predict the mass spectrum, dissociations in field-free regions (metastable decompositions), and isotope effects in the fragmentations of propane and propane-*1,1-*$^2H_2$ ions. However, they also stated "No choice of frequencies and energies ... consistent with present experimental evidence and knowledge of activated complex structures gave a sufficiently low value for the rate of CH bond break." Vestal[3] used improved state-counting methods to reasonably predict the propane mass spectrum by the QET. However, to predict observable field free region losses of an H atom and $CH_4$, very "loose" configurations of the propane ion had to be assumed, configurations justifiable only because they gave good agreement between experiment and theory. Lifshitz and Shapiro[5] determined experimental rate constants for field free region dissociations of the propane ion; they obtained $k = 3.2 \times 10^4\ s^{-1}$ for $C_3H_8^{+\bullet} \rightarrow C_2H_4^{+\bullet} + CH_4$.

In a 1967 photoionization study that included propane, Chupka and Berkowitz[6] found that $C_3H_7^+$ production is strongly reduced by competition from $C_2H_4^{+\bullet}$ formation, competition much stronger even than predicted by Vestal with the QET.[3] This is very surprising, because in general, simple cleavages with low threshold are expected to be the dominant reactions at all energies, and H atom loss from ionized propane (a simple bond cleavage) has a lower appearance energy (AE) than that of the quickly favored $C_2H_4^{+\bullet}$ formation (i.e., $AE(C_3H_7^+) = 11.59$ eV, $AE(C_2H_4^{+\bullet}) = 11.72$.eV).[6] The latter would also be expected to be relatively slowed by a more constrained transition state. Although Vestal utilized a loose transition state for $C_2H_4^{+\bullet}$ formation to explain this competition pattern, Chupka and Berkowitz concluded that it is $C_3H_7^+$ formation that has an unusual dependence on internal energy. To rationalize the suppression of $C_3H_7^+$ at higher energies, they suggested that the reaction involves a rigid transition state, possibly one yielding a ringlike structure more stable than *s*-$C_3H_7^+$.

Vestal and Futrell[4] calculated minimum rate constants of $6.3 \times 10^5\ s^{-1}$ for H atom loss and $1.1 \times 10^6\ s^{-1}$ for $CH_4$ elimination from the propane ion. However, to obtain these values, they made the transition state for H atom loss from ionized propane a tight ringlike structure, the "tightest transition state used in the propane ion calculation" and chose a similar, but slightly

† University of Texas Medical Branch.
‡ Universitat de Barcelona.
§ CSIC.
⊥ E-mail: olivella@taga.qo.ub.es.

10.1021/jp982856k CCC: $15.00 
Published on Web 12/03/1998

looser, transition state for $CH_4$ elimination. Also, Stockbauer and Inghram[7] later concluded on the basis of the comparison of QET predictions and experimental results that H atom loss from ionized propane does not give *s*-$C_3H_7^+$, and that a ring structure must be considered for the transition state of the H atom loss. However, after the early studies of the losses of H atom and $CH_4$ from the propane ion, *s*-$C_3H_7^+$ was demonstrated to be the stable propyl ion isomer,[8−10] suggesting that the transition state for loss of the secondary H atom is not cyclic. In addition, recent high level ab initio calculations[11] demonstrated that the $CH_4$ elimination from the propane ion involves the formation of a H-bridged $C_2H_5^+-CH_3^\bullet$ ion−neutral complex, which undergoes a H-transfer between the two partners. The formation of this ion−neutral complex is the rate-determining step of the $CH_4$ elimination and is characterized by a transition state looking like a methyl radical coordinated to a distorted classical ethyl cation, which is quite different from the transition states assumed by early workers.[2−4] Thus, despite a long history, it is unclear that the Rice−Rampsberger−Kassel−Marcus (RRKM)/QET theory has been adequately applied to the decompositions of the propane ion. In light of the role of the dissociations of ionized propane in the development of the QET and the persistent uncertainties in its application to those reactions, we undertook combined ab initio and RRKM calculations to study the losses of H atom, $CH_3^\bullet$, and $CH_4$ from ionized propane. These calculations reasonably reproduced the pattern of experimental observations, demonstrating the applicability of the RRKM/QET approach to this system.

## Ab Initio Computational Details

The geometries of the relevant stationary points on the $C_3H_8^{+\bullet}$ ground state PES were located at the full (i.e., not frozen core) second-order Møller−Plesset perturbation theory[12] employing the split-valence d-polarized 6-31G(d) basis set.[13] The amount of spin contamination in the reference spin-unrestricted Hartree−Fock (UHF)[14] wave function of the doublet states was found to be very small; thus the expectation values of the $\hat{S}^2$ operator were always very close to the value of 0.75 for a pure doublet state, i.e., in a range of 0.7586−0.7641. To characterize the stationary points as minima or as saddle points and to facilitate zero-point vibrational energy (ZPVE) corrections to the relative energies, the harmonic vibrational frequencies were obtained at the UMP2/6-31G(d) level by diagonalizing the mass-weighted Cartesian force constant matrix. To predict more reliable ZPVE values, the raw UMP2/6-31G(d) harmonic vibrational frequencies were scaled by 0.93 to account for their average overestimation at this level of theory.[15] Absolute entropies were obtained, assuming ideal gas behavior, from the scaled harmonic frequencies and moments of inertia by standard methods.[16]

Equilibrium structures were fully optimized within appropriate symmetry constraints using analytical gradient methods.[17] Starting geometries for the transition-structure optimizations were obtained by the usual reaction-coordinate method, the energy being minimized with respect to all other geometrical variables for successive increments in the reaction coordinate. The approximate transition structures located in this way were refined by minimizing the scalar gradient of the energy, using Schlegel's algorithm.[17] The optimized geometries were checked for the correct number of imaginary eigenvalues of the force constant matrix.

At geometries optimized using the UMP2/6-31G(d) wave function, the energies were recalculated using (frozen core) QCISD with a perturbative estimation of the triples (QCISD(T)) method[18] employing the double d,p-polarized triple split-valence 6-311G(2d,2p) basis set.[19] To see if diffuse functions might be important in describing cation−molecule interactions, the QCISD(T) calculations were also carried out with the 6-311+G(2d,2p) basis set, which includes a single additional diffuse sp shell on heavy atoms only.[20] There was little difference in the energy changes calculated using the two basis sets, and only the energies derived from the latter are reported. Our best relative energies correspond to the QCISD(T)/6-311+G(2d,2p) level together with the ZPVE correction calculated at the UMP2/6-31G(d) level. Unless otherwise noted, relative energies in the text refer to this overall level of theory.

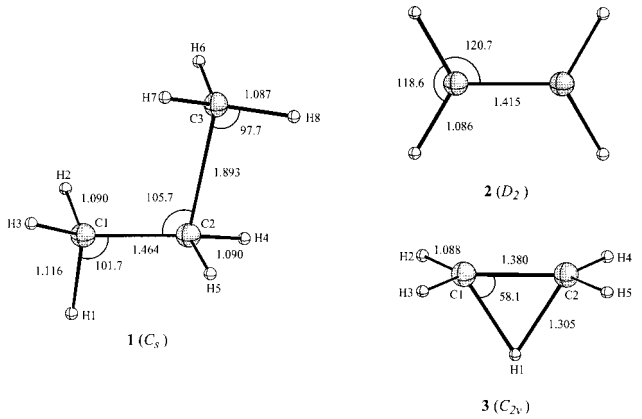


**Figure 1.** UMP2/6-31G(d)-optimized geometries of the equilibrium structures of the propane radical cation (**1**), the ethene radical cation (**2**), and the ethyl cation (**3**).

All of the ab initio calculations described here were performed with the GAUSSIAN 92 and GAUSSIAN 94 program packages,[21] running on a HP9000 J280/2 workstation and on the IBM SP2 computer at the Centre de Supercomputacio de Catalunya (CESCA) in Barcelona.

## Results and Discussion of the ab Initio Calculations

The optimized molecular geometries and calculated total energies for the equilibrium structures of $C_3H_8^{+\bullet}$ (**1**), $C_2H_4^{+\bullet}$ (**2**), $C_2H_5^+$ (**3**), and the transition structure for the rate-determining step of the methane elimination from ionized propane (**TS12**) have been reported previously.[11] For the sake of completeness these structures are given in Figures 1 and 2 (bond lengths in angstroms and bond angles in degrees). The most relevant geometrical parameters of the optimized molecular structures involved in the H atom loss from **1** are given in Figures 3 and 4 (bond lengths in angstroms and bond angles in degrees).[22] Our previous study[11] on the unimolecular decomposition reactions of **1** revealed that the loss of $CH_3^\bullet$ takes place through a reaction path involving a steady increase of the energy along the CC bond elongation, leading to the sum of the energies of the separated dissociation fragments, $CH_3^\bullet$ and $C_2H_5^+$. Therefore, it was concluded that the $CH_3^\bullet$ loss from **1** does not involve any transition structure (i.e., there is no intrinsic potential energy barrier for the reverse association reaction of the dissociation fragments). Total energies calculated at various levels of theory for all species involved in the present study are given in Table 1, which includes the ZPVE and the absolute entropies at 298 K computed from the scaled vibrational frequencies. The relative energies of the stationary points on the potential energy surface associated to the losses of the H atom, $CH_4$, and $CH_3^\bullet$ from **1** are collected in Table 2.

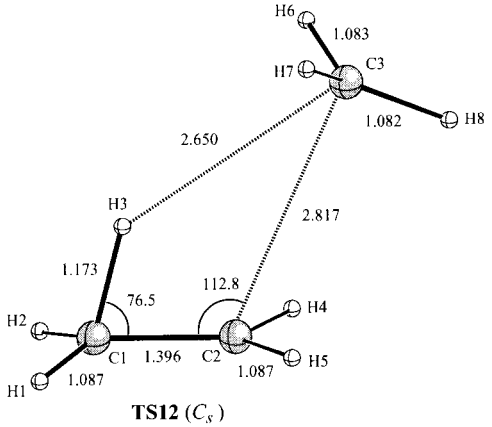


**TS12** ($C_s$)

**Figure 2.** UMP2/6-31G(d)-optimized geometry of the transition structures for the rate-determining step of the methane elimination from ionized propane.

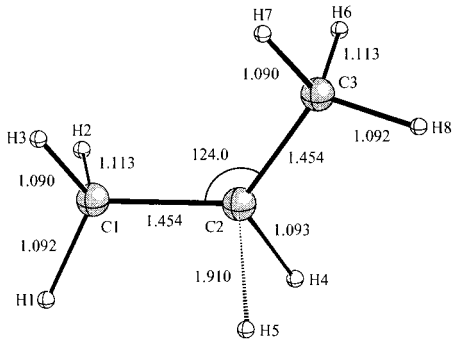


**TS14** ($C_1$)

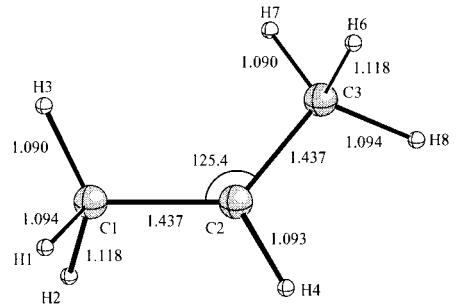


**4** ($C_2$)

**Figure 3.** UMP2/6-31G(d)-optimized geometries of the transition structure (**TS14**) for the H atom loss from ionized propane leading to the formation of the *sec*-propyl cation and the equilibrium structure of the *sec*-propyl cation (**4**).

Experimental data derived from known heats of formation or appearance energy measurements are also given in Table 2.

**Formation of the *sec*-Propyl Cation.** The H atom loss from ionized propane leading to the formation of the *sec*-propyl cation was simulated by stretching the C2−H5 bond of **1** systematically in steps of 0.1 Å and optimizing all other geometry parameters. The increase of the C2−H5 distance caused a simultaneous shortening of the C2−C3 bond. This path led to the approximate location of a saddle point at C2−H5 = 1.91 Å. The structure located in this way was optimized using Schlegel's algorithm. The resulting stationary point, **TS14** (Figure 3), was characterized as a true transition structure by checking that it had only one imaginary harmonic vibrational frequency (535i $cm^{-1}$). The activation energy at 0 K for the H atom loss from ionized propane via the transition structure **TS14** is predicted to be 75 kJ/mol, which is somewhat above the critical energy of 62 kJ/mol (0.64 eV) determined as the difference between the AE of 11.59 ± 0.01 eV for production of $C_3H_7^+$ from propane measured by Chupka and Berkowitz[6] and the recommended propane adiabatic ionization potential of 10.95 ± 0.05 eV.[23] Further elongation of the C2−H5 distance in **TS14** led to the dissociation fragments *sec*-propyl cation and H atom. The equilibrium structure calculated for the *sec*-propyl cation (**4**) is displayed in Figure 3. The sum of the energies of the separated fragments, **4** and an H atom, lies 73 kJ/mol above the energy of **1**. This 0 K dissociation energy is in reasonably good agreement with the experimental estimate of 65 kJ/mol determined from 0 K heats of formation.[23]

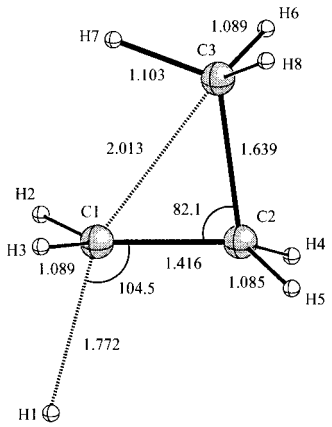


**TS15** ($C_s$)

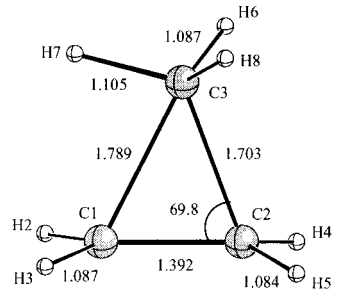


**5** ($C_s$)

**Figure 4.** UMP2/6-31G(d)-optimized geometries of the transition structure (**TS15**) for the H atom loss from ionized propane leading to the formation of corner-protonated cyclopropane and the equilibrium structure of corner-protonated cyclopropane (**5**).

**Formation of the Corner-Protonated Cyclopropane.** The H atom loss from ionized propane leading to the formation of *n*-propyl cation was simulated by stretching the C1−H1 bond of **1** systematically in steps of 0.1 Å and optimizing all other geometry parameters. The increase of the C1−H1 distance caused a simultaneous shortening of the C1−C2, C2−C3, and C3−C1 distances accompanied by the rotation of the $CH_3$ group around the C3−C2 bond. This path led to the approximate location of a saddle point at C1−H1 = 1.77 Å showing $C_s$ molecular symmetry. The structure located in this way was optimized using Schlegel's algorithm. The resulting stationary point, **TS15** (Figure 4), was characterized as a true transition structure by checking that it had only one imaginary harmonic vibrational frequency (878i $cm^{-1}$). It is worth noting that the elongation of any of the other C1−H or C3−H bonds in **1** led

**TABLE 1: Calculated Total Energies (Hartrees), Zero-Point Vibrational Energies (ZPVE, kJ/mol),[a] and Absolute Entropies (*S*, J Mol$^{-1}$ K$^{-1}$)[a,b] for UMP2/6-31G(d) Optimized Structures**

| structure | point group | state | nivf[c] | UMP2/6-31G(d) | QCISD[d]/ 6-311+G(2d,2p) | QCISD(T)[d]/ 6-311+G(2d,2p) | ZPVE | *S* |
|---|---|---|---|---|---|---|---|---|
| **1** | $C_s$ | $^2$A′ | 0 | −118.27906 | −118.44568 | −118.46190 | 246 | 296 |
| **2** | $D_2$ | $^2$B$_1$ | 0 | −77.92651 | −78.01589 | −78.02410 | 123 | 239 |
| **3** | $C_{2v}$ | $^1$A$_1$ | 0 | −78.56145 | −78.66193 | −78.67303 | 154 | 228 |
| **4** | $C_2$ | $^1$A | 0 | −117.76065 | −117.90801 | −117.92496 | 222 | 274 |
| **5** | $C_s$ | $^1$A′ | 0 | −117.75358 | −117.89469 | −117.91360 | 230 | 272 |
| $CH_4$ | $T_d$ | $^1$A$_1$ | 0 | −40.33704 | −40.41468 | −40.42005 | 113 | 186 |
| $CH_3^•$ | $D_{3h}$ | $^2$A$_2$″ | 0 | −39.67303 | −39.74128 | −39.74531 | 75 | 196 |
| H | | $^2$S | | −0.49823 | −0.49981 | −0.49981 | 0 | 115 |
| **TS12** | $C_s$ | $^2$A′ | 1 | −118.24060 | −118.40998 | −118.42559 | 233 | 331 |
| **TS14** | $C_1$ | $^2$A | 1 | −118.25535 | −118.40980 | −118.42694 | 229 | 291 |
| **TS15** | $C_s$ | $^2$A | 1 | −118.24171 | −118.39359 | −118.41270 | 235 | 287 |

[a] Calculated using UMP2/6-31G(d) harmonic vibrational frequencies, scaled by 0.93. [b] At 298 K and 1 atm. [c] Number of imaginary vibrational frequencies. [d] In the frozen core approximation.

**TABLE 2: Calculated Relative Energies (kJ/mol) for UMP2/6-31G(d)-Optimized Stationary Points on the $C_3H_8^{•+}$ Potential Energy Surface**

| stationary point | UMP2/ 6-31G(d) | QCISD[a]/ 6-311+G (2d,2p) | QCISD(T)[a]/ 6-311+G (2d,2p) | QCISD(T)[a]/ 6-311+G (2d,2p) + ZPVE | exp |
|---|---|---|---|---|---|
| **1** | 0 | 0 | 0 | 0 | |
| **2** + $CH_4$ | 41 | 40 | 47 | 37 | 41[b] |
| **3** + $CH_3^•$ | 117 | 112 | 114 | 97 | 97[c] |
| **4** + H | 53 | 99 | 97 | 73 | 65[d] |
| **5** + H | 72 | 134 | 127 | 111 | 97[d] |
| **TS12** | 101 | 94 | 95 | 82 | 74[e] |
| **TS14** | 62 | 94 | 92 | 75 | 62[e] |
| **TS15** | 98 | 137 | 129 | 118 | |

[a] In the frozen core approximation. [b] Estimated from 0 K heats of formation: $\Delta H_f(CH_2{=}CH_2^{•+}) = 1074$,[23] $\Delta H_f(CH_4) = -67$,[23] and $\Delta H_f(CH_3CH_2CH_3^{•+}) = 966$ kJ/mol at 0 K. The last value was obtained by combining $\Delta H_f(CH_3CH_2CH_3) = -90$ kJ/mol at 0 K[23] and the propane adiabatic ionization potential of 10.95 ± 0.05 eV.[23] [c] Estimated from 0 K heats of formation: $\Delta H_f(C_2H_5^+) = 914$,[12] $\Delta H_f(CH_3^•) = 149$,[23] and $\Delta H_f(CH_3CH_2CH_3^{•+}) = 966$[23] kJ/mol. [d] Estimated from thermochemical data.[23] [e] Estimated from the appearance potentials.[6]

to the location of the same transition structure **TS15**. The activation energy at 0 K for the H atom loss from ionized propane via the transition structure **TS15** is predicted to be 118 kJ/mol, which is 43 kJ/mol higher than the one calculated for the H atom loss via the transition structure **TS14**. This predicts little loss of H atoms other than one of those linked to the middle carbon atom in ionized propane, in accordance with experimental observations when isotope effects and H-interchange prior to dissociation are taken into account.[5,7] Further elongation of the C1−H1 distance in **TS15** led to the dissociation of ionized propane to the corner-protonated cyclopropane and an H atom. The equilibrium structure (**5**) calculated for the corner-protonated cyclopropane is displayed in Figure 4. The sum of the energies of the separated fragments, **5** and an H atom, lies 111 kJ/mol above the energy of **1**. The calculated energy difference between the *sec*-propyl cation **4** and the corner-protonated cyclopropane form of the $C_3H_7^+$ ion (**5**) is 38 kJ/mol, in good agreement with the experimental value of 35 kJ/mol.[24] Earlier MP4(SDQ)/6-31G(d,p) calculations with HF/6-31G(d) optimized geometries predicted a value of 34 kJ/mol for this difference.[10]

## RRKM Computational Details

For H atom, $CH_3^•$, and $CH_4$ losses from ionized propane, the dependence of the unimolecular rate constant $k(E)$ on the internal energy excess with respect to the ground state energy including ZPVE of the reactant ion, $E$, was initially calculated on the basis of standard RRKM theory of unimolecular reactions, which can be formulated as[25]

$$k(E) = \frac{W^\dagger(E - E_0)}{h\rho(E)} \quad (1)$$

where $E_0$ is the critical energy of the reaction (i.e., the energy barrier including the ZPVE), $W^\dagger(E - E_0)$ is the total number of states of the transition state within the energy interval $E - E_0$, $\rho(E)$ is the density of states of the reactant ion, and $h$ is Planck's constant. $W^\dagger(E - E_0)$ and $\rho(E)$ were enumerated by direct count of vibrational states using a program[26] based on the Beyer−Swinehart algorithm.[27]

The RRKM computations employed the potential energy barriers calculated at the QCISD(T)/6-31+G(2d,2p) level and the UMP2/6-31G(d)-calculated harmonic vibrational frequencies scaled by the factor 0.93. The torsional modes were treated as low-frequency vibrations. For H atom loss, the relative energy of 75 kJ/mol calculated for **TS14** was taken as the critical energy and the harmonic vibrational frequencies calculated for this structure were taken as the transition state frequencies. For $CH_4$ elimination, the relative energy of 82 kJ/mol calculated for the rate-determining transition structure **TS12** was taken as the critical energy for the overall reaction and the harmonic vibrational frequencies calculated for this transition structure were taken as the transition state frequencies. Since the $CH_3^•$ loss from ionized propane does not involve any transition structure (i.e., the reverse association reaction is barrierless),[11] the sum of the relative energies of the separated dissociation fragments **3** and $CH_3^•$ (97 kJ/mol) was taken as the critical energy of this reaction, whereas the harmonic vibrational frequencies calculated for a propane ion structure with the C2−C3 bond elongated to 3.4 Å and all other geometry parameters optimized, **6** (Figure 5), were taken as the vibrational frequencies of the effective transition state. Such a choice of the C2−C3 distance was made in order to obtain an energy difference between the crossover points of the curve for the $C_2H_4^{+•}$ ion with the curves for the *s*-$C_3H_7^+$ and $C_2H_5^+$ ions in the RRKM-calculated breakdown graph close enough to experimental results. Tables S1−S4 (Supporting Information) contain the UMP2/6-31G(d)-calculated harmonic vibrational frequencies and their description for **1**, **TS14**, **TS12**, and **6**.

In addition, quantum-mechanical barrier tunneling (QMBT) correction to the rate constants was considered in the RRKM calculations. To incorporate QMBT effects in the framework

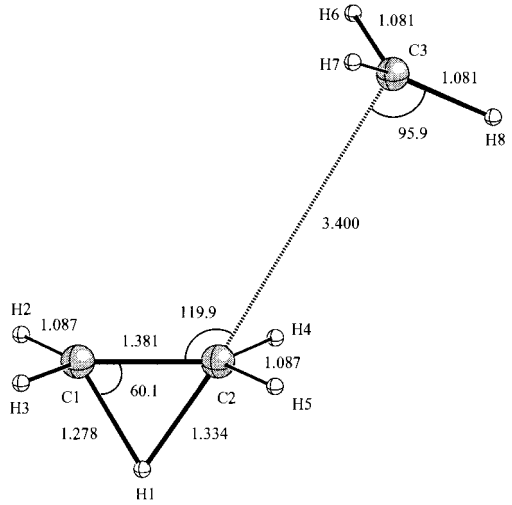


**6** ($C_s$)

**Figure 5.** Structure used for computing the harmonic vibrational frequencies of the effective transition state for the methyl radical loss from ionized propane.

of the RRKM theory,[28] $W^{\dagger}(E - E_0)$ in eq 1 was replaced by $W_{QM}{}^{\dagger}(E - E_0)$:

$$W^{\dagger}_{QM}(E - E_0) = \sum_n P(E - \epsilon_n{}^{\dagger}) \qquad (2)$$

where $P(E - \epsilon_n{}^{\dagger})$ is the one-dimensional tunneling probability as a function of the energy $E$ in the reaction coordinate and $\epsilon_n{}^{\dagger}$ is the vibrational energy levels of the transition state; in the classical limit of no tunneling $W_{QM}{}^{\dagger}(E - E_0) \rightarrow W^{\dagger}(E - E_0)$. The barrier along the reaction coordinate was approximated by a generalized Eckart potential.[29] In the case of the loss of an H atom, it is worth noticing that the sum of the energies of the dissociation fragments are calculated to lie high (73 kJ/mol) above the energy of **1**. Since quantum-mechanical tunneling through an energy barrier between reactants and products cannot take place at energies below the energy of the product, it follows that the **1** → **4** + H dissociation begins at an energy nearly identical to the sum of the energies of the corresponding dissociation fragments, which is only 2 kJ/mol below the calculated energy barrier of 75 kJ/mol. Consequently, the calculated QMBT corrections to the rate constants for the H atom loss were negligible. For the same reasons, the calculated QMBT corrections to the rate constants for the $CH_3^{\bullet}$ loss were also found to be negligible. In light of these findings, we decided finally not to consider QMBT corrections to the rate constants of the latter two dissociations in the RRKM calculations.

## Results and Discussion of the RRKM Calculations

The logarithm of $k(E)$ versus $E$ curves for the losses of H atom, $CH_4$, and $CH_3^{\bullet}$ from propane ion, calculated by using eqs 1 and 2, are shown in Figure 6. The breakdown graphs for ionized propane, depicting relative abundances of the $C_3H_8{}^{+\bullet}$, $s$-$C_3H_7{}^{+}$, $C_2H_4{}^{+\bullet}$, and $C_2H_5{}^{+}$ ions as a function of $E$ at $10^{-5}$ s after ionization, are displayed in Figure 7. The curves were obtained by integrating the rate equations using the rate constants shown in Figure 6.

The RRKM-calculated rate constants reproduce the experimental dominance of H atom loss at lowest energies, its rapid replacement by $CH_4$ elimination with increasing energy, and the dominance of $CH_3^{\bullet}$ loss at still higher energies (Figure 7).

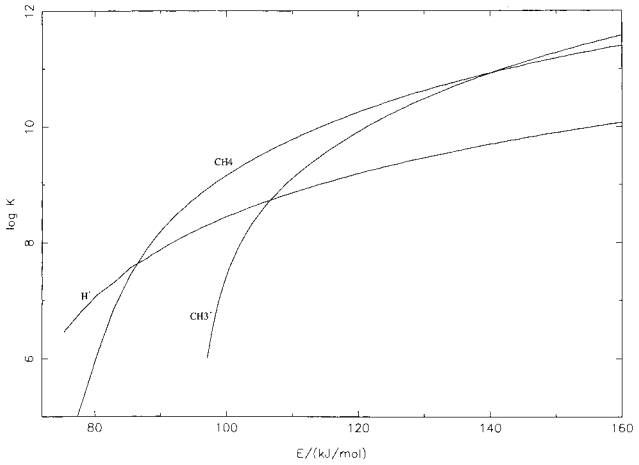


**Figure 6.** Plots of the logarithm of the RRKM-derived rate constant, $k(E)$, versus internal energy excess with respect the ZPVE of the propane radical cation, $E$, for the losses of an H atom, $CH_4$, and $CH_3^{\bullet}$ from ionized propane.

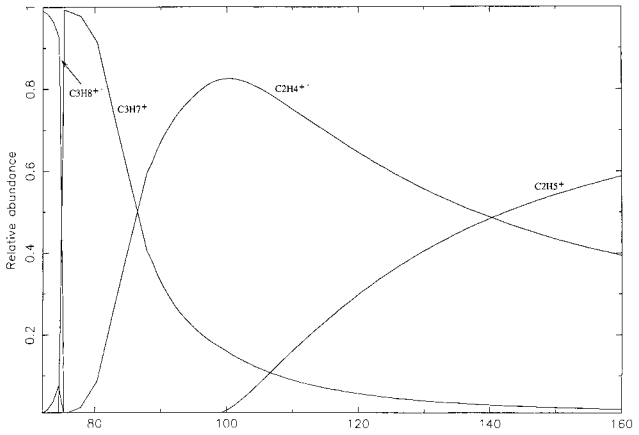


**Figure 7.** Breakdown graphs for the ionized propane depicting the relative abundances of the $C_3H_8{}^{+\bullet}$, $s$-$C_3H_7{}^{+}$, $C_2H_4{}^{+\bullet}$, and $C_2H_5{}^{+}$ ions as a function of internal energy excess with respect the ZPVE of the propane radical cation, $E$, at $10^{-5}$ s after ionization. The curves were obtained by integrating the rate equations using rate constants shown in Figure 6.

According to RRKM theory, at a given internal energy $E$ the rate of a reaction with a critical energy $E_0$ is proportional to the ratio between the $W^{\dagger}(E - E_0)$ of the transition state and $\rho(E)$ of the reactant (eq 1). $W^{\dagger}(E - E_0)$ is the number of possible (vibrational) states of the transition state within the energy interval $E - E_0$, which in turn, is inversely related to the values of the vibrational frequencies in the transition state; that is, the lower the transition state frequencies, the larger the number of possible states. In the case of competing reactions (i.e., the possible reactions of a given reactant) $\rho(E)$ is the same for all of them, so the relative rate constants are determined by the critical energies of the reactions and the respective transition state vibrational frequencies. The propane ion is the reactant in all three of the reactions being compared, so the relative rates of those reactions at internal energies substantially above their critical energies are determined largely by the transition state vibrational frequencies. On going from the reactant to the respective transition state in all three of the reactions, it is reasonable to assume that the vibrational frequencies of the propane ion are transformed into the frequencies of the transition state (i.e., the transition, state frequencies are related to the propane ion ones). Thus at high internal energies, the rate constants for H atom, $CH_3^{\bullet}$, and $CH_4$ losses from the propane

**TABLE 3: Energy Differences (kJ/mol) Between Crossover Points in the Breakdown Graphs for the Ionized Propane**

| $C_3H_7^+$ [a] | $C_2H_4^{+\bullet}$ [b] | source |
|---|---|---|
| 11.5 | 53.5 | this work |
| 12.6 | 50.2 | ref 6 |
| 15.9 | 50.2 | ref 7 |
| 24.7 | 54.7 | ref 30 |

[a] Crossover of curve for $C_3H_7^+$ with those for $C_3H_8^{+\bullet}$. [b] Crossover of curve for $C_2H_4^{+\bullet}$ with those for $C_3H_7^+$ and $C_2H_5^+$.

ion are determined by the lowering of the vibrational frequencies on going from the reactant to the respective transition state.

Differences between the energies of the crossover points for competing processes in experimental and RRKM-calculated breakdown graphs are given in Table 3. The crossover of the $C_3H_7^+$ curve with the corresponding $C_3H_8^{+\bullet}$ and $C_2H_4^{+\bullet}$ curves are 11.5 kJ/mol apart, and experimental differences[6,7,30] are 12.6, 15.9, and 24.7 kJ/mol. Experiment and RRKM calculations agree reasonably in light of the variation in the experimental values. The RRKM calculations place the crossing points of the $CH_4$ elimination curve with the other curves 53.5 kJ/mol apart as compared to experimental differences[6,7,30] of 50.2, 50.2, and 54.7 kJ/mol.

**Hydrogen Atom Loss.** Because stretching of a CH bond is primarily involved in the loss of a H atom from the middle carbon, except for the vibrational mode that becomes the transition vector (i.e., the vector describing the nuclear motion associated to the transition state imaginary frequency), the frequencies in the transition state for that process are quite similar to those for the propane ion. Comparing the vibrational frequencies given in Tables S1 and S2 (Supporting Information), it is found that some frequencies increased and some decreased on going from the propane ion to the transition state for the H atom loss. Furthermore, the changes that do occur are in the range in which there is little effect on rate constant, namely the moderate to high frequency range. The numerator in eq 1 increases very slowly beyond a few kJ/mol above threshold with increasing internal energy, producing a rather slow increase in the rate constant of this reaction with increasing internal energy. Thus it is simply the absence of low frequencies in the transition state for loss of the H atom rather than any unusual feature of the transition state, such as cyclization, that produces the relatively slow rise in the rate constant of this reaction with increasing internal energy.

Kropf and co-workers[2] used rounded off and grouped propane vibrational frequencies for the propane ion and modified those frequencies to represent the transition state. For the propane ion they assumed two $CH_3$ free rotations, motions that instead have frequencies of 188 and 268 $cm^{-1}$ in **1** according to our ab initio calculations. For the H atom loss the only change they made on going from the propane ion to the transition state was to convert a high-frequency CH stretch (3000 $cm^{-1}$) to the transition vector. As would be predicted by the above discussion, their RRKM calculations also gave a slow rise in the rate constant of H atom loss with increasing energy. Vestal and Futrell[4] used frequencies similar to those of Kropf and co-workers for the propane ion and the transition state. These choices of transition vector and preservation of frequencies between the reactant and the transition state are in accord with our ab initio calculations, although the assumption of free rotations in the propane ion is not. Vestal[3] used the frequencies of Kropf and co-workers[2] with some modifications to describe H atom loss from the propane ion. He retained a CH stretch as the transition vector, but in addition he reduced a $CH_3$ rocking frequency from 1000 to 100 $cm^{-1}$ in that transition state and in some RRKM calculations made the free rotors in the propane ion low frequency torsions. Our ab initio calculations indicate the presence of low frequency torsions rather than free rotors in the reactant and transition state and do not support Vestal's reduced $CH_3$ rocking frequency in the transition state.

**Methane Elimination.** As described previously,[11] the transition state for the rate-determining step in the $CH_4$ elimination from the propane ion is a loosely associated methyl radical−ethyl ion complex; i.e., the elongated CC bond in the propane ion is stretched further and the methyl is moved toward the H atom it will abstract (Figure 2). A bending mode of the propane ion involving one hydrogen atom on each methyl is considered to become the transition vector. The latter is a combination of CCC bending, methyl wagging of the two hydrogen atoms tightly bound to C1, and C2−C3 stretching. Although a number of vibrational frequencies are significantly lowered upon forming this transition state (Table S3, Supporting Information), the lowest frequency in the transition state for $CH_4$ elimination (38 $cm^{-1}$) arises from easier torsional motion around the elongated C2−C3 bond, which corresponds to the lowest frequency (188 $cm^{-1}$) in the propane ion. Other frequencies that significantly decrease are the CCC bending (216 to 153 $cm^{-1}$), C1−C2 torsion (268 to 203 $cm^{-1}$), the C2−C3 stretching (453 to 211 $cm^{-1}$), CH bending in the loose methyl (643 to 319 $cm^{-1}$), and a combined C1−C2 torsion-CH bending (1310 to 911 $cm^{-1}$). There are not increased frequencies, as might be expected for formation of a more ordered transition state. The lack of increased frequencies is attributed to CC bond-breaking dominating in the transition state (Figure 2), with H-transfer taking place in a separate second step.[11] Vibrational frequencies are considerably lowered in the rate-determining transition state because H-transfer is not yet very far along. The decreases in vibrational frequencies make the rate-determining transition state for $CH_4$ elimination "looser" than that for H atom loss. This feature is supported by the activation entropies of +35 and −5 J $mol^{-1}$ $K^{-1}$ for $CH_4$ elimination and H atom loss, respectively, obtained from the calculated absolute entropies at 298 K (Table 1).[31] As a consequence of the substantial reduction of the lowest frequencies of the propane ion in the transition state, the $CH_4$ elimination rises much more rapidly in rate constant with increasing internal energy than the H atom loss, the reaction that is favored just above its threshold. This noncompetitiveness of a simple bond cleavage is interesting, as complex-mediated alkane eliminations are usually overwhelmed by simple dissociations involving cleavage of the same CC bond at higher energies.[32−36]

Kropf and co-workers[2] used a CC stretching as the vibrational mode that becomes the transition vector for $CH_4$ elimination, in contrast to our assignment of a methyl bending motion as the precursor to the transition vector. For the transition state, they also increased a CC stretching frequency from 900 to 1200 $cm^{-1}$, changed two assumed propane ion $CH_3$ free rotations to 500 $cm^{-1}$ vibrational frequencies, and reduced two $CH_3$ rocking frequencies from 1000 to 100 $cm^{-1}$. Vestal[3] assumed one free rotor in the transition state and none or two in the propane ion, with little change in frequencies otherwise between the reactant and the transition state. Vestal and Futrell[4] tightened the transition state for this process mainly by stopping two free rotors. None of the previously assumed transition states is very much like the one we obtained from ab initio calculations.

QMBT effects are predicted to produce some elimination of $CH_4$ below the calculated activation energy at 0 K for this reaction (82 kJ/mol) and to slightly increase the competitiveness of $CH_4$ elimination with H atom loss just above the threshold

for the former. Thus QMBT effects should enhance the loss of $CH_4$ by metastable decomposition. However, our predicted contribution of QMBT effects to the rate constant of $CH_4$ loss above the top of the barrier is small, so QMBT effects are not the major factor causing $CH_4$ elimination to overcome H atom loss with increasing internal energy.

**Methyl Radical Loss.** The transition vector for $CH_3^\bullet$ loss involves stretching of the CC bond that is already elongated in the propane ion. As in the case of the $CH_4$ elimination, a number of vibrational frequencies are significantly lowered upon forming the transition state (Table S4, Supporting Information). The lowest frequency in the effective transition state for the $CH_3^\bullet$ loss arises from easier torsional motion of the C3-methyl group around the elongated C2−C3 bond, which corresponds to the lowest frequency (188 $cm^{-1}$) in the propane ion. However, in the effective transition state for the $CH_3^\bullet$ loss this frequency is lowered to a value (16 $cm^{-1}$), which is about a half of its value (38 $cm^{-1}$) in the transition state for the $CH_4$ elimination. This causes the rate constant of the $CH_3^\bullet$ loss to rise much more rapidly with energy than those for the first two reactions, in accord with experimental observations. Other frequencies that significantly decrease are the CCC bending (216 to 67 $cm^{-1}$) and two CH bendings in the loose methyl group (643 to 201 and 731 to 197 $cm^{-1}$). A low vibrational frequency of 79 $cm^{-1}$, which corresponds to a torsional motion around the C1−C2 bond of the loose methyl group taken as a whole, is generated in the effective transition state for the $CH_3^\bullet$ loss. Most of the lowering of frequencies comes from the extreme weakening of the C2−C3 bond. Interestingly, a C1-methyl group torsion around the C1−C2 bond increases from 268 to 1190 $cm^{-1}$, a change attributable to stiffening of the torsion in forming the bridged $C_2H_5^+$ ion. Our description of $CH_3^\bullet$ loss differs from previous ones[2−4] primarily in not having free rotors in the propane ion. Our higher frequencies for the propane ion torsion relative to the previously used values permits more loosening of these torsions on going to the transition state.

The rapid replacement of complex-mediated $CH_4$ elimination by the associated dissociation in our RRKM calculations reproduces the often-observed rapid replacement of alkane eliminations by associated alkyl radical loss with increasing energy.[32−36] In contrast to the H atom loss, it is also in accord with the venerable generalization that bond cleavages increase in rate constant much more rapidly with increasing internal energy than reactions with complex transition states.

## Conclusions

Present work shows that the RRKM/QET approach adequately describes the unimolecular decompositions of the propane ion, including the slow rise of the rate constant of the H atom loss with internal energy, when transition states found by means of high level ab initio calculations are used. The absence of motions other than the stretch in the transition vector of the transition states for losses of single atoms causes little change to occur in the vibrational frequencies on going from the reactant to the transition state other than that for the transition vector. This predicts that the rate constants for such reactions will usually increase more slowly with internal energy than those of most competitive reactions.

**Acknowledgment.** The work in Barcelona was supported by the Spanish DGICYT (Grant PB95-0278-C02-01). We acknowledge the University of Barcelona for partial allocations of computing time in the Centre de Supercomputacio de Catalunya (CESCA).

**Supporting Information Available:** Tables S1−S4 summarizing the UMP2/6-31G(d)-calculated harmonic vibrational frequencies and their description for **1**, **TS14**, **TS12**, and **6** (8 pages). See any current masthead page for ordering and Internet access instructions.

## References and Notes

(1) Rosenstock, H. M.; Wallenstein, M. B.; Wahrhaftig, A. L.; Eyring, H. *Proc. Natl. Acad. Sci. U.S.A.* **1952**, *38*, 667.

(2) Kropf, A.; Eyring, E. M.; Wahrhaftig, A. L.; Eyring, H. *J. Chem. Phys.* **1960**, *32*, 149.

(3) Vestal, M. *J. Chem. Phys.* **1965**, *43*, 1356.

(4) Vestal, M.; Futrell, J. H. *J. Chem. Phys.* **1970**, *52*, 978.

(5) Lifshitz, C.; Shapiro, M. *J. Chem. Phys.* **1966**, *45*, 4242.

(6) Chupka, W. A.; Berkowitz, J. *J. Chem. Phys.* **1967**, *47*, 2921.

(7) Stockbauer, R.; Inghram, M. G. *J. Chem. Phys.* **1976**, *65*, 4081.

(8) McAdoo, D. J.; McLafferty, F. W.; Bente, P. F., III. *J. Am. Chem. Soc.* **1972**, *94*, 2027.

(9) Koch, W.; Liu, B. *J. Am. Chem. Soc.* **1989**, *111*, 3479.

(10) Raghavachari, K.; Whiteside, R. A.; Pople, J. A.; Schleyer, P. v. *J. Am. Chem. Soc.* **1981**, *103*, 5649.

(11) Olivella, S.; Solé, A.; McAdoo, D. J. *J. Am. Chem. Soc.* **1996**, *118*, 9368.

(12) (a) Møller, C.; Plesset, M. *Phys. Rev.* **1934**, *46*, 618. (b) Pople, J. A.; Binkley, J. S.; Seeger, R. *Int. J. Quantum Chem., Symp.* **1976**, *10*, 1.

(13) Hariharan, P. C.; Pople, J. A. *Theor. Chim. Acta* **1973**, *28*, 213.

(14) Pople, J. A.; Nesbet, R. K. *J. Chem. Phys.* **1954**, *22*, 571.

(15) (a) Hout, R. F.; Levi, B. A.; Hehre, W. J. *J. Comput. Chem.* **1982**, *3*, 234. (b) DeFrees, D. J.; McLean, A. D. *J. Chem. Phys.* **1985**, *82*, 333.

(16) See, e.g.: McQuarrie, D. *Statistical Mechanics;* Harper and Row: New York, 1986.

(17) Schlegel, H. B. *J. Comput. Chem.* **1982**, *3*, 214.

(18) Pople, J. A.; Head-Gordon, M.; Raghavachari, K. *J. Chem. Phys.* **1987**, *87*, 5968.

(19) Frisch, M. J.; Pople, J. A.; Binkley, J. S. *J. Chem. Phys.* **1984**, *80*, 3265.

(20) Hehre, W. J.; Radom, L.; Schleyer, P. v. R.; Pople, J. A. *Ab Initio Molecular Orbital Theory*; John Wiley: New York, 1986; pp 86−87.

(21) Frisch, M. J.; Trucks, G. W.; Schlegel, H. B.; Gill, P. M. W.; Johnson, B. G.; Robb, M. A.; Cheeseman, J. R.; Keith, T. A.; Petersson, G. A.; Montgomery, J. A.; Raghavachari, K.; Al-Laham, M. A.; Zakrzewski, V. G.; Ortiz, J. V.; Foresman, J. B.; Cioslowski, J.; Stefanov, A.; Nanayakkara, A.; Challacombe, M.; Peng, C. Y.; Ayala, P. Y.; Chen, W.; Wong, M. W.; Andres, J. L.; Replogle, E. S.; Gomperts, R.; Martin, R. L.; Fox, D. J.; Binkley, J. S.; Defrees, D. J.; Baker, J.; Stewart, J. J. P.; Head-Gordon, M.; Gonzalez, C.; Pople, J. A. *GAUSSIAN 94*; Gaussian, Inc.: Pittsburgh, PA, 1995.

(22) Full sets of Cartesian coordinates for all optimized molecular geometries are available upon request from S.O.

(23) Lias, S. G.; Bartmess, J. E.; Liebman, J. B.; Holmes, J. L.; Levin, R. D.; Mallard, W. G. *J. Phys. Chem. Ref. Data* **1988**, *17*, 168.

(24) (a) Chong, S. L.; Franklin, J. L. *J. Am. Chem. Soc.* **1972**, *94*, 6347. (b) Viviani, D.; Levy, J. B. *Int. J. Chem. Kinet.* **1979**, *11*, 1021. (c) Attina, M.; Cacace, F.; Giacomello, P. *J. Am. Chem. Soc.* **1980**, *102*, 4768.

(25) Gilbert, R. G.; Smith, S. C. *Theory of Unimolecular and Recombination Reactions*; Blackwell Scientific Publications: Oxford, U.K., 1990.

(26) Solé, A. Unpublished work.

(27) Beyer, T.; Swinehart, D. F. *Commun. Assoc. Comput. Machines* **1973**, *16*, 379.

(28) (a) Miller, W. H. *J. Am. Chem. Soc.* **1979**, *101*, 6810. (b) Garrett, B. C.; Truhlar, D. G. *J. Phys. Chem.* **1979**, *83*, 1079.

(29) Johnston, H. S.; *Gas-Phase Reaction Rate Theory*; Ronald Press: New York, 1966.

(30) Gilman, J. P.; Hsieh, T.; Meisels, G. G. *J. Chem. Phys.* **1982**, *76*, 3497.

(31) Benson, S. W. *Thermochemical Kinetics;* John Wiley: New York, 1976; p 86.

(32) Hudson, C. E.; McAdoo, D. J. *Int. J. Mass Spectrom. Ion Processes* **1984**, *59*, 325.

(33) Traeger, J. C.; Hudson, C. E.; McAdoo, D. J. *J. Phys. Chem.* **1988**, *92*, 1519.

(34) McAdoo, D. J.; Traeger, J. C.; Hudson, C. E.; Griffin, L. L. *J. Phys. Chem.* **1988**, *92*, 1524.

(35) Heinrich, N.; Louage, F.; Lifshitz, C.; Schwarz, H. *J. Am. Chem. Soc.* **1988**, *10*, 8183.

(36) Olivella, S.; Solé, A.; McAdoo, D. J.; Griffin, L. L. *J. Am. Chem. Soc.* **1995**, *117*, 2557.